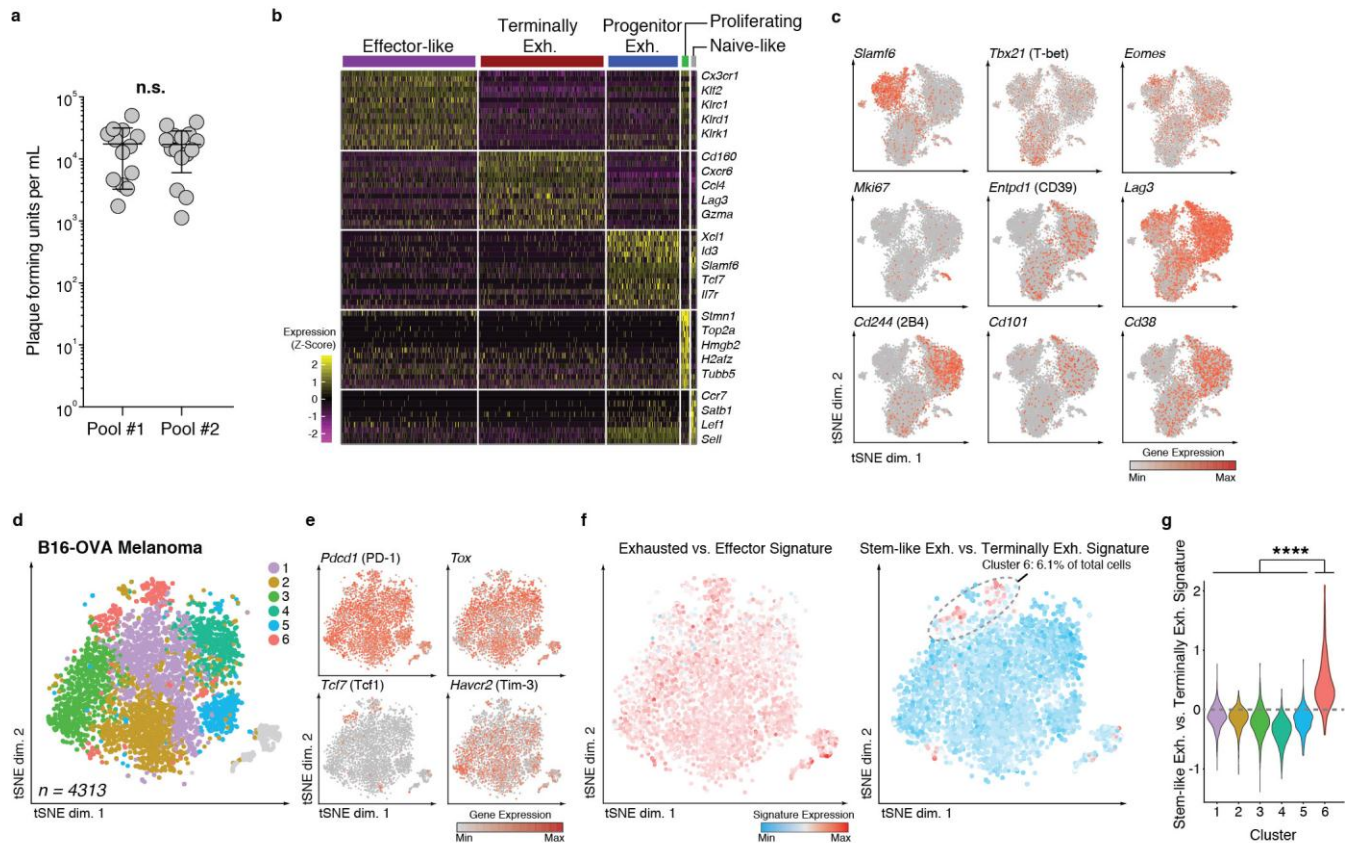


In the format provided by the authors and unedited.

Subsets of exhausted CD8⁺ T cells differentially mediate tumor control and respond to checkpoint blockade

Brian C. Miller ^{1,2,3,4,5,10}, Debattama R. Sen ^{1,3,6,10}, Rose Al Abosy ^{1,3}, Kevin Bi ^{1,3}, Yamini V. Virkud⁷, Martin W. LaFleur ^{1,3,4,5,6}, Kathleen B. Yates^{1,3}, Ana Lako⁸, Kristen Felt⁸, Girish S. Naik⁸, Michael Manos^{2,8}, Evisa Gjini^{2,8}, Juhi R. Kuchroo^{4,5,6}, Jeffrey J. Ishizuka^{1,2,3}, Jenna L. Collier ^{1,3,4,5,6}, Gabriel K. Griffin^{1,3,9}, Seth Maleri^{4,5}, Dawn E. Comstock^{1,3,6}, Sarah A. Weiss^{1,3,6}, Flavian D. Brown^{1,3,4,5,6}, Arpit Panda^{1,3}, Margaret D. Zimmer³, Robert T. Manguso³, F. Stephen Hodi^{2,8}, Scott J. Rodig^{8,9}, Arlene H. Sharpe^{3,4,5,6} and W. Nicholas Haining ^{1,3,6*}

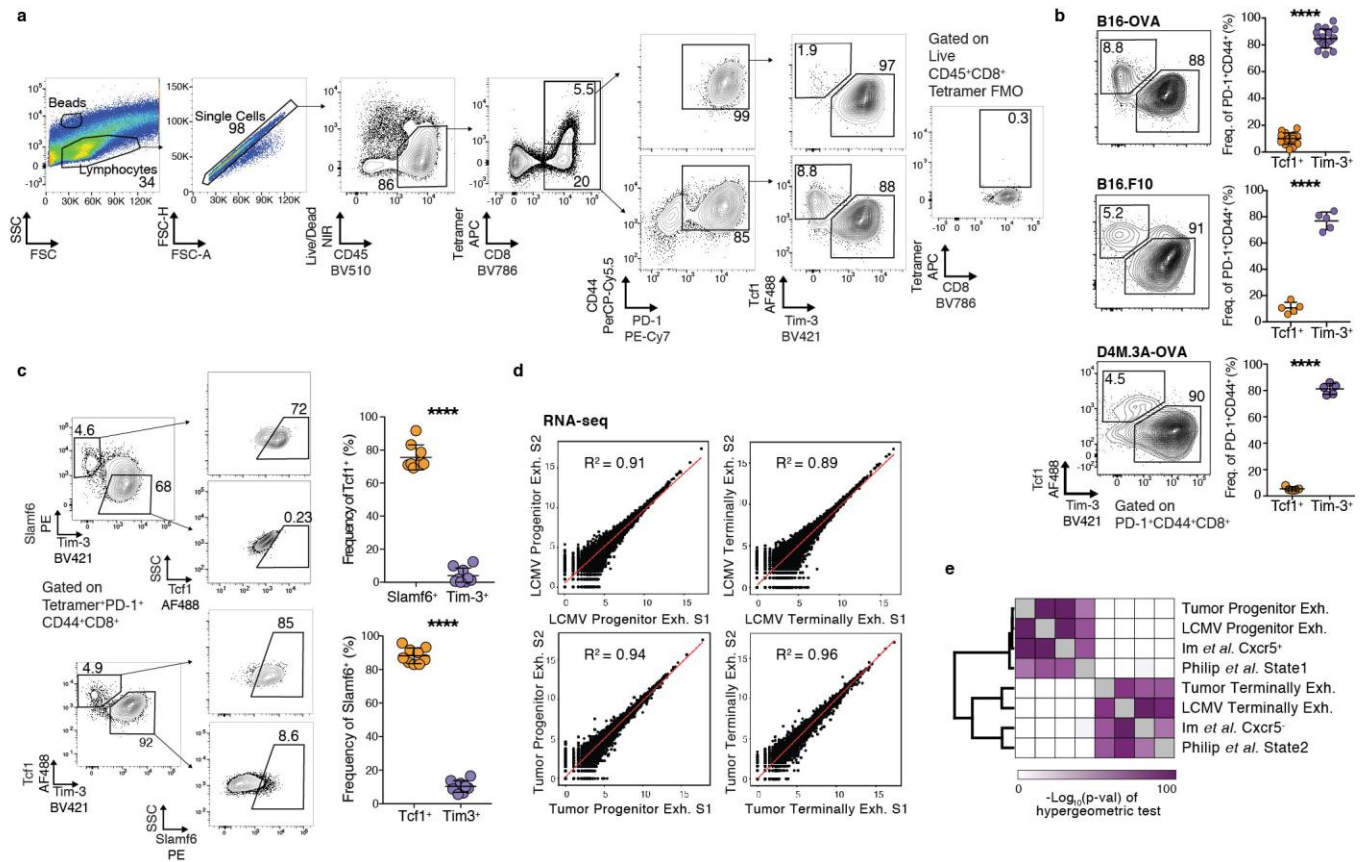
¹Department of Pediatric Oncology, Dana-Farber Cancer Institute, Boston, MA, USA. ²Department of Medical Oncology, Dana-Farber Cancer Institute, Boston, MA, USA. ³Broad Institute of MIT and Harvard, Cambridge, MA, USA. ⁴Evergrande Center for Immunologic Diseases, Harvard Medical School and Brigham and Women's Hospital, Boston, MA, USA. ⁵Department of Immunology, Blavatnik Institute, Harvard Medical School, Boston, MA, USA. ⁶Division of Medical Sciences, Harvard Medical School, Boston, MA, USA. ⁷Division of Pediatric Allergy and Immunology, Massachusetts General Hospital, Boston, MA, USA. ⁸Center for Immuno-Oncology, Dana-Farber Cancer Institute, Boston, MA, USA. ⁹Department of Pathology, Brigham and Women's Hospital, Boston, MA, USA. ¹⁰These authors contributed equally: Brian C. Miller, Debattama R. Sen. *e-mail: wnhaining@gmail.com



Supplementary Figure 1

Similar populations of progenitor exhausted CD8⁺ T cells identified in chronic viral infection and mouse tumors by single-cell RNA-seq.

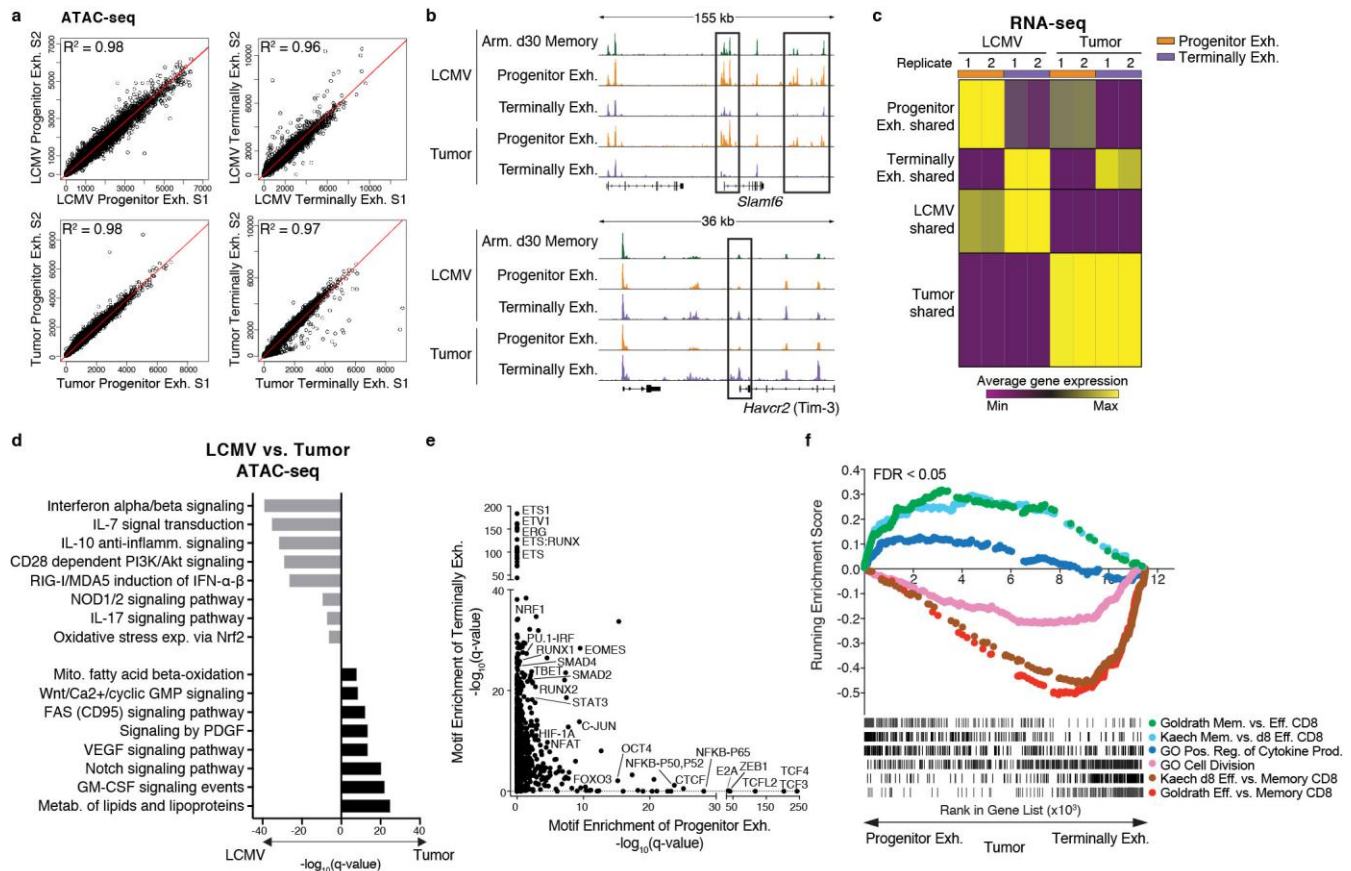
a, Serum viral titers of LCMV Clone 13 infected mice pooled to generate single-cell RNA-seq data, $n = 13$ (pool 1) or 15 (pool 2) mice. **b**, Heat map of top differentially expressed genes in each cluster, with key transcripts highlighted on the right. Groups colored according to clustering (Fig. 1a). **c**, Expression of indicated genes overlaid on LCMV CD8⁺ T cell tSNE projection of 9,194 single cells (Fig. 1a). **d**, tSNE projection of single-cell RNA-seq profiles from 4,313 SIINFEKL tetramer⁺ CD8⁺ T cells from day 20 B16-OVA tumors colored by cluster. Unlabeled cluster in grey represents cell doublets. **e**, Expression of indicated genes overlaid on tSNE projection from **d**. **f**, Enrichment of a signature of genes upregulated in exhausted vs. effector CD8⁺ T cells (GSE9650) or stem-like exhausted vs. terminally exhausted CD8⁺ T cells (GSE84105). **g**, Violin plots of the enrichment score of the gene signature derived from stem-like exhausted vs. terminally exhausted CD8⁺ T cells (GSE84105) for each cell cluster in Supplementary Fig. 1d, $n > 263$ single cells per cluster. Mean \pm s.d. (**a**), two-sided Student's t test (**a**), two-sided Kolmogorov-Smirnov test (**g**); n.s. $p > 0.05$, **** $p \leq 0.0001$



Supplementary Figure 2

Progenitor exhausted and terminally exhausted CD8⁺ T cell populations confirmed in multiple mouse tumor models by flow cytometry.

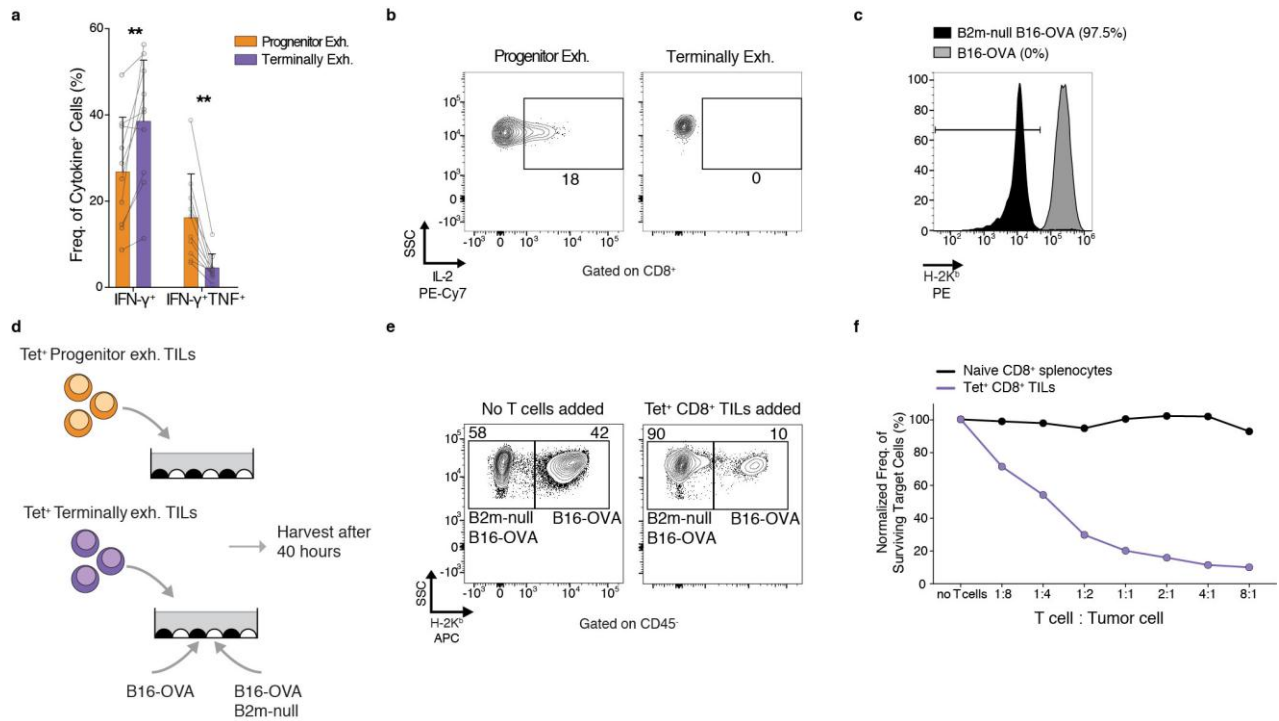
a, Representative flow cytometry gating strategy for progenitor and terminally exhausted cells (left) with tetramer full-minus one (FMO, right). **b**, Frequency of progenitor exhausted (Tcf1⁺Tim-3⁻) and terminally exhausted (Tcf1⁺Tim-3⁺) CD8⁺ T cells from B16-OVA tumors (top), B16.F10 tumors (middle) or D4M.3A-OVA tumors (bottom) gated on PD-1⁺CD44⁺ cells. Representative flow plot (left) and summary (right) of three independent experiments, n = 17 mice (B16-OVA), n = 5 mice (B16.F10), or one of two independent experiments, n = 5 mice (D4M.3A-OVA). **c**, Frequency of Tcf1⁺ cells within Slamf6⁺Tim-3⁻ or Slamf6⁻Tim-3⁺ cells (top) or frequency of Slamf6⁺ cells within Tcf1⁺Tim-3⁻ or Tcf1⁻Tim-3⁺ cells (bottom) from B16-OVA tumors. Representative flow plots (left) and summary (right) of one of two independent experiments, n = 9 mice. **d**, Scatter plot of transcript abundance (log₁₀) between replicates for all 13,012 transcripts. **e**, Hypergeometric overlap of gene expression profiles from progenitor exhausted or terminally exhausted gene signatures from LCMV or TILs with expression data from indicated cell states from the literature, top 150 differentially expressed transcripts used for comparison. Mean +/- s.d. (**b,c**), two-sided Student's t test (**b,c**); two-sided hypergeometric test (**e**); **** p ≤ 0.0001



Supplementary Figure 3

Progenitor and terminally exhausted CD8⁺ TILs have distinct epigenetic and transcriptional features.

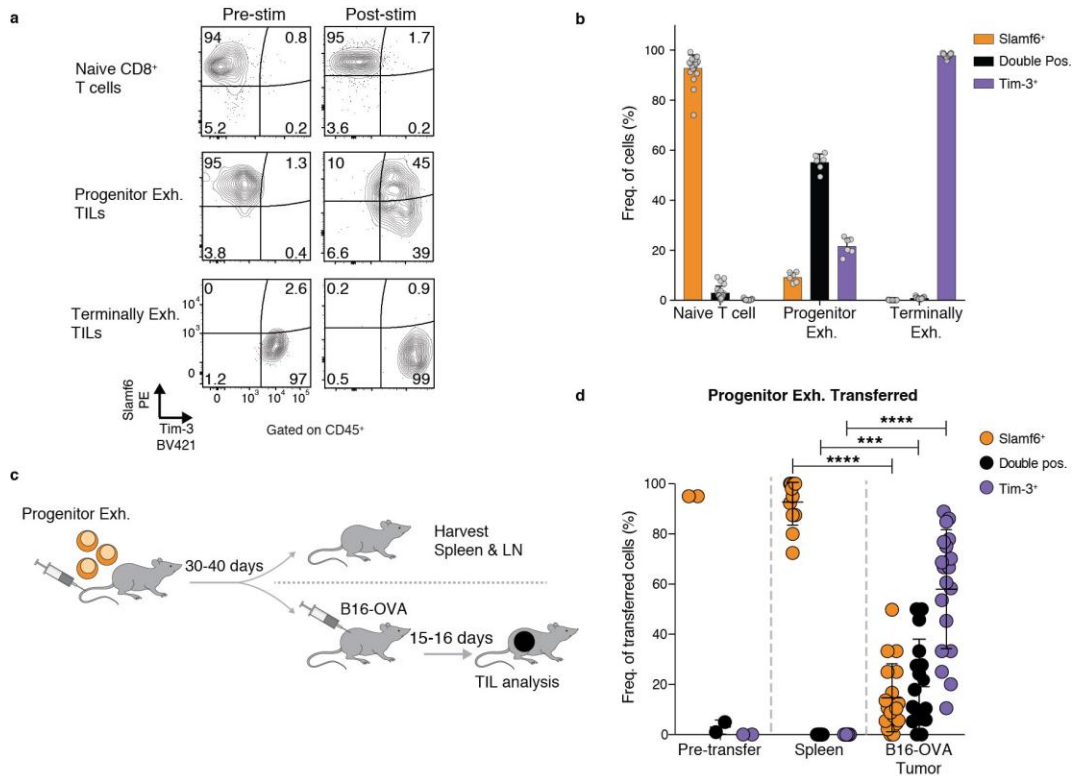
a, Scatter plot of normalized chromatin accessibility between replicates at each peak for all 67,221 peaks. **b**, Representative ATAC-seq tracks at the *Slamf6* (top) and *Havcr2* (bottom) loci. **c**, Heatmap showing average mRNA expression of neighboring genes within each cluster (Fig. 2e) in each cell state. **d**, Enrichment of gene signatures from MSigDB (rows) from cluster of regions in LCMV C13 or tumor (Fig. 2e). Q-values (hypergeometric test) presented as $-\log_{10}$. All ATAC-seq data representative of two biologically independent pooled samples. **e**, Scatter plot of differential motif enrichment in progenitor exhausted or terminally exhausted cluster. X and Y axis represent $-\log_{10}$ of q-value (hypergeometric test). **f**, GSEA of signatures in the ranked list of genes differentially expressed by progenitor exhausted vs. terminally exhausted CD8⁺ T cells from B16-OVA tumors. All RNA-seq data representative of two biologically independent pooled samples. FDR < 0.05 for each comparison by gene set permutation test.



Supplementary Figure 4

Progenitor exhausted and terminally exhausted CD8⁺ TILs have distinct functional properties.

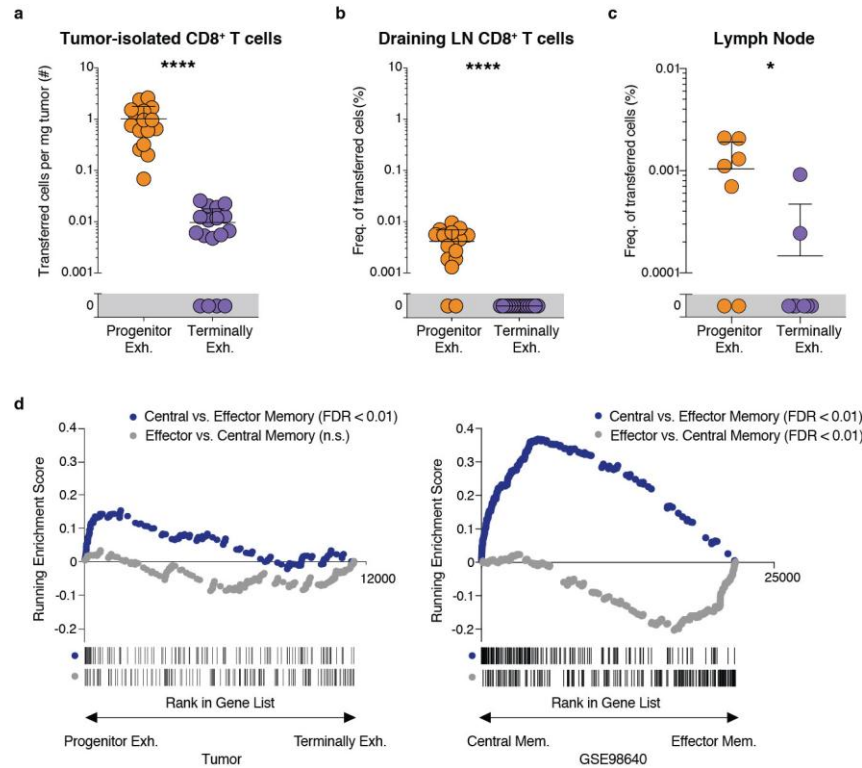
a, Frequency of IFN- γ ⁺ and IFN- γ ⁺TNF⁺ progenitor exhausted (Tcf1⁺Tim-3⁻) or terminally exhausted (Tcf1⁻Tim-3⁺) TILs stimulated for 6 hours *ex vivo* with PMA and ionomycin. Summary of one of two independent experiments, n = 10 mice. **b**, Representative flow plots of IL-2 production from progenitor exhausted or terminally exhausted TILs stimulated for 6 hours *ex vivo* with PMA and ionomycin, n = 3 independent wells. **c**, Representative histograms of H-2K^b expression on B16-OVA and B2m-null B16-OVA cells after 24 hours *in vitro* IFN- γ stimulation from one experiment. Percentage of cells within indicated gate shown. **d**, Schema of experimental design for *in vitro* killing assay. **e**, Representative flow plots of tumor cells after 40 hour co-culture with no T cells (left) or tetramer⁺ CD8⁺ TILs (right) stained against H-2K^b. **f**, Frequency of surviving target cells (B16-OVA) to control cells (B2m-null B16-OVA) normalized to no T cell wells. One of three independent experiments, n = 2 independent wells per condition. Mean +/- s.d. (**a**); two-sided Student's paired t test (**a**); ** p \leq 0.01



Supplementary Figure 5

Progenitor exhausted CD8⁺ T cells differentiate into terminally exhausted CD8⁺ T cells.

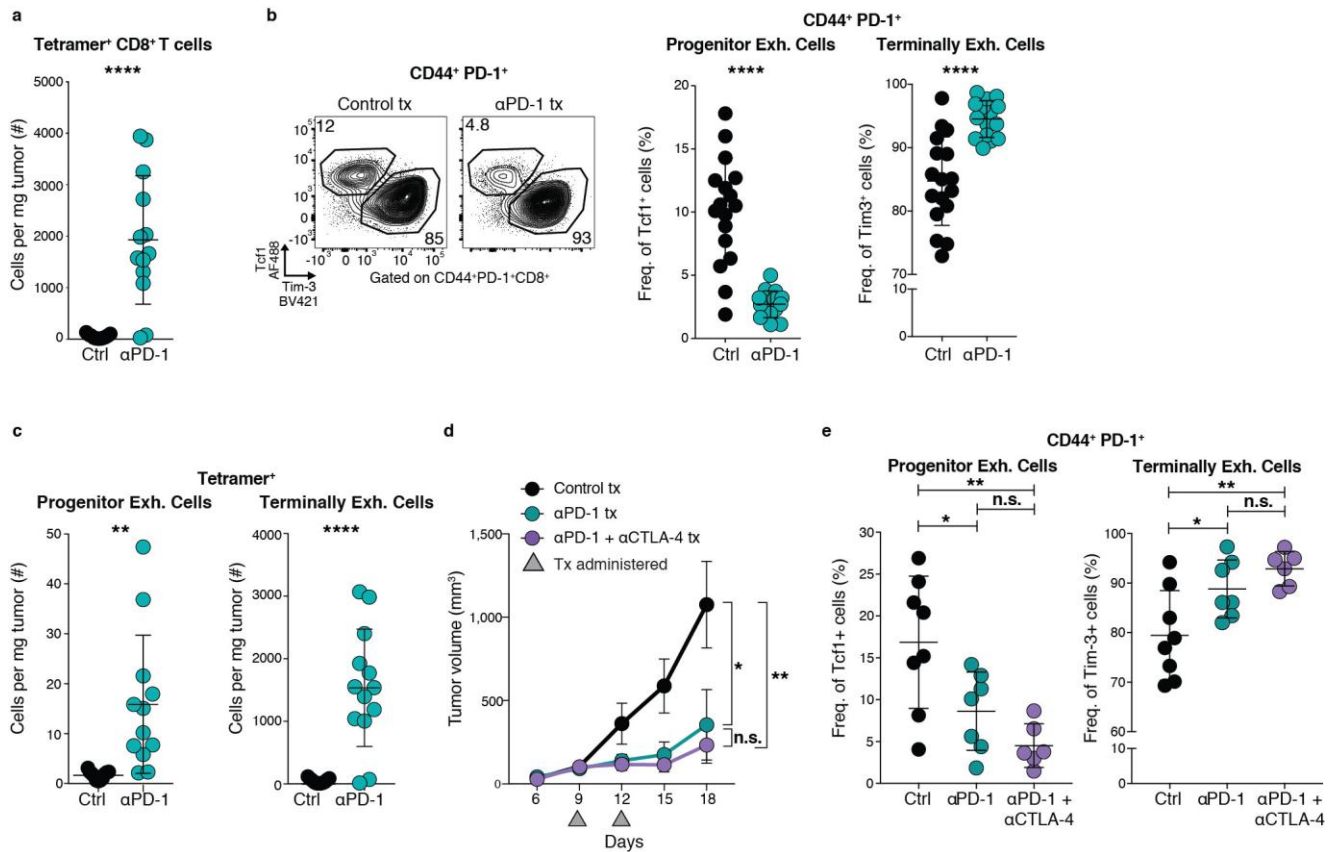
a, Representative flow plots of the cell surface phenotype of naive CD8⁺ splenocytes, progenitor exhausted TILs, or terminally exhausted TILs pre-stim (left) or after 40 hours co-culture with tumor cells (right) in the *in vitro* cytotoxicity assay (Supplementary Fig. 4d). **b**, Summary of the phenotype of tetramer⁺ sorted T cells after 40 hours co-culture with tumor cells. One of three independent experiments, n = 6 (progenitor exh.) or 21 (naive and terminally exh.) independent wells. **c**, Schema of experimental design for *in vivo* persistence and tumor assays. **d**, Summary of the phenotype of transferred progenitor exhausted cells harvested from spleen or tumors. Summary of two independent experiments, n = 9 (spleen) or 16 (tumor) mice post-transfer.



Supplementary Figure 6

Progenitor exhausted CD8⁺ T cells have increased persistence compared with terminally exhausted CD8⁺ T cells.

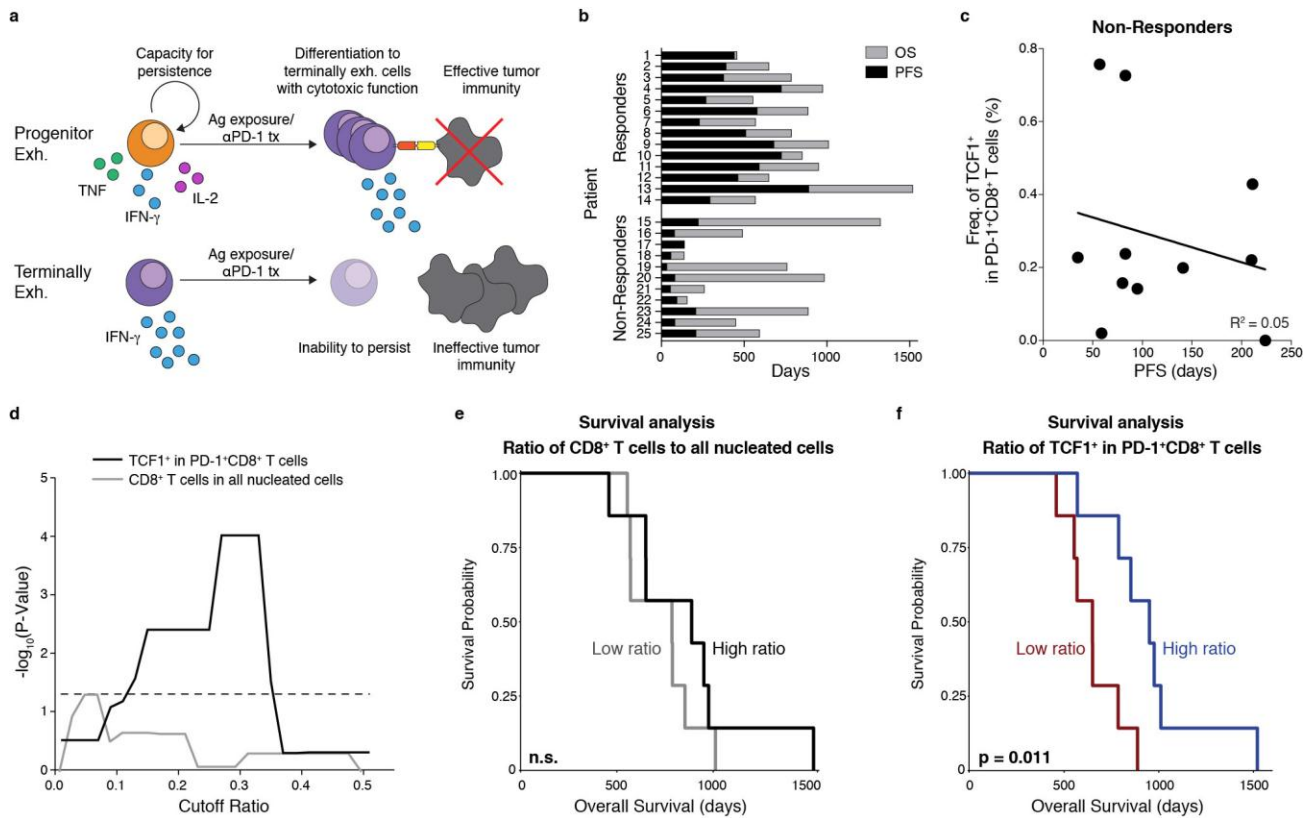
a, Cell numbers/mg tumor of transferred (CD45.2⁺) progenitor or terminally exhausted cells in recipient tumors. Summary of two of three independent experiments, n = 16 (progenitor exh.) or 17 (terminally exh.) mice. **b**, Frequency of transferred progenitor exhausted or terminally exhausted cells in draining lymph nodes of recipient mice. Summary of two independent experiments, n = 16 (progenitor exh.) or 17 (terminally exh.) mice. **c**, Frequency of transferred progenitor or terminally exhausted cells in lymph nodes from *in vivo* persistence assay mice without tumor implantation (Supplementary Fig. 5c). Summary of two independent experiments, n = 7 mice. **d**, GSEA of central vs. effector memory signature (GSE23321) in the ranked list of genes differentially expressed by progenitor exhausted vs. terminally exhausted from B16-OVA tumors (left) or ranked list of genes differentially expressed by a second, independent dataset of central memory versus effector memory cells (GSE98640), for comparison. FDR shown for each comparison calculated by gene set permutation test. Mean +/- s.d. (**a-c**); two-sided Student's t test (**a-c**); * p ≤ 0.05, **** p ≤ 0.0001



Supplementary Figure 7

Treatment with anti-PD-1 or combination anti-PD-1 + anti-CTLA-4 increases the relative abundance of terminally exhausted cells in the tumor.

a, Cell number/mg tumor of total tetramer⁺ CD8⁺ T cells from isotype control or anti-PD-1 treated B16-OVA tumors. Summary of two independent experiments, n = 13 mice. **b**, Frequency of progenitor exhausted (Tcf1⁺Tim-3⁻) and terminally exhausted (Tcf1⁺Tim-3⁺) PD-1⁺CD44⁺ CD8⁺ T cells from isotype control or anti-PD-1 treated B16-OVA tumors. Representative flow plots (left) and summary (right) of three independent experiments, n = 17 (control tx) or 15 (anti-PD-1 tx) mice. **c**, Cell number/mg tumor of progenitor exhausted and terminally exhausted CD8⁺ T cells from isotype control or anti-PD-1 treated B16-OVA tumors, gated on tetramer⁺ cells. Summary of two independent experiments, n = 13 mice. **d**, Growth curves of B16-OVA tumors treated with 100μg anti-PD-1 +/- 100μg anti-CTLA-4 or isotype control antibodies on days 9 and 12. One of two representative experiments, n = 6 mice (anti-PD-1 + anti-CDTL-4 tx), 7 mice (anti-PD-1 tx), or 8 mice (control tx). **e**, Summary of the frequency of progenitor exhausted and terminally exhausted cells from one of two representative experiments, n = 6 mice (anti-PD-1 + anti-CDTL-4 tx), 7 mice (anti-PD-1 tx), or 8 mice (control tx). Mean +/- s.e.m. (**d**); Mean +/- s.d. (**a-c**, **e**); two-sided Student's t test (**a-e**); n.s. p > 0.05, * p ≤ 0.05, ** p ≤ 0.01, **** p ≤ 0.0001



Supplementary Figure 8

Increased fraction of progenitor exhausted CD8⁺ T cells is associated with duration of response to checkpoint blockade in patients with advanced melanoma.

a, Diagram of the functions of progenitor exhausted and terminally exhausted CD8⁺ T cells in the tumor microenvironment. **b**, Swimmer plots of 25 patients with advanced melanoma who received nivolumab (anti-PD-1) and ipilimumab (anti-CTLA-4) showing progression free survival and overall survival. **c**, Frequency of progenitor exhausted cells in all activated/exhausted cells plotted against progression-free survival (days) in patients without durable clinical benefit (non-responders, n = 11). Linear regression line shown. **d**, Graph plotting the significance value from survival analysis for different cutoff ratios of TCF1⁺ in PD-1⁺CD8⁺ T cells (black line) or CD8⁺ T cells in all nucleated cells (grey line), from 0 to max ratio in responders (n = 14). Dotted line at $p = 0.05$. **e,f**, Kaplan-Meier curves of overall survival in responders (n = 14) by high vs. low percentage of total CD8⁺ T cells in all nucleated cells (**e**, cutoff at median 7.6%) or by percentage of progenitor exhausted cells (TCF1⁺) in all activated/exhausted CD8⁺ T cells (**f**, cutoff at median 14.9%). two-sided Likelihood ratio test (**d-f**); n.s. $p > 0.05$